



The WFIRST Coronagraph Instrument

*John Trauger, on behalf of CGI project science
Jet Propulsion Laboratory, California Institute of Technology*

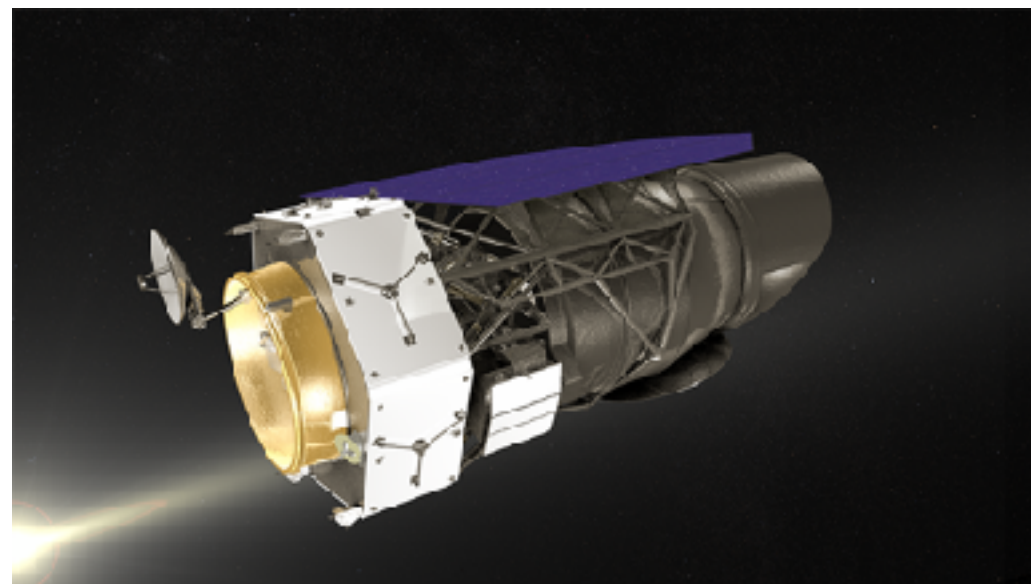
*KISS-MPIA Workshop
for the Direct Detection and Characterization of Exoplanets
Caltech, 9 April 2018*

The decision to implement the WFIRST mission will not be finalized until NASA completes the National Environmental Policy Act (NEPA) process. This document is being made available for information purposes only.

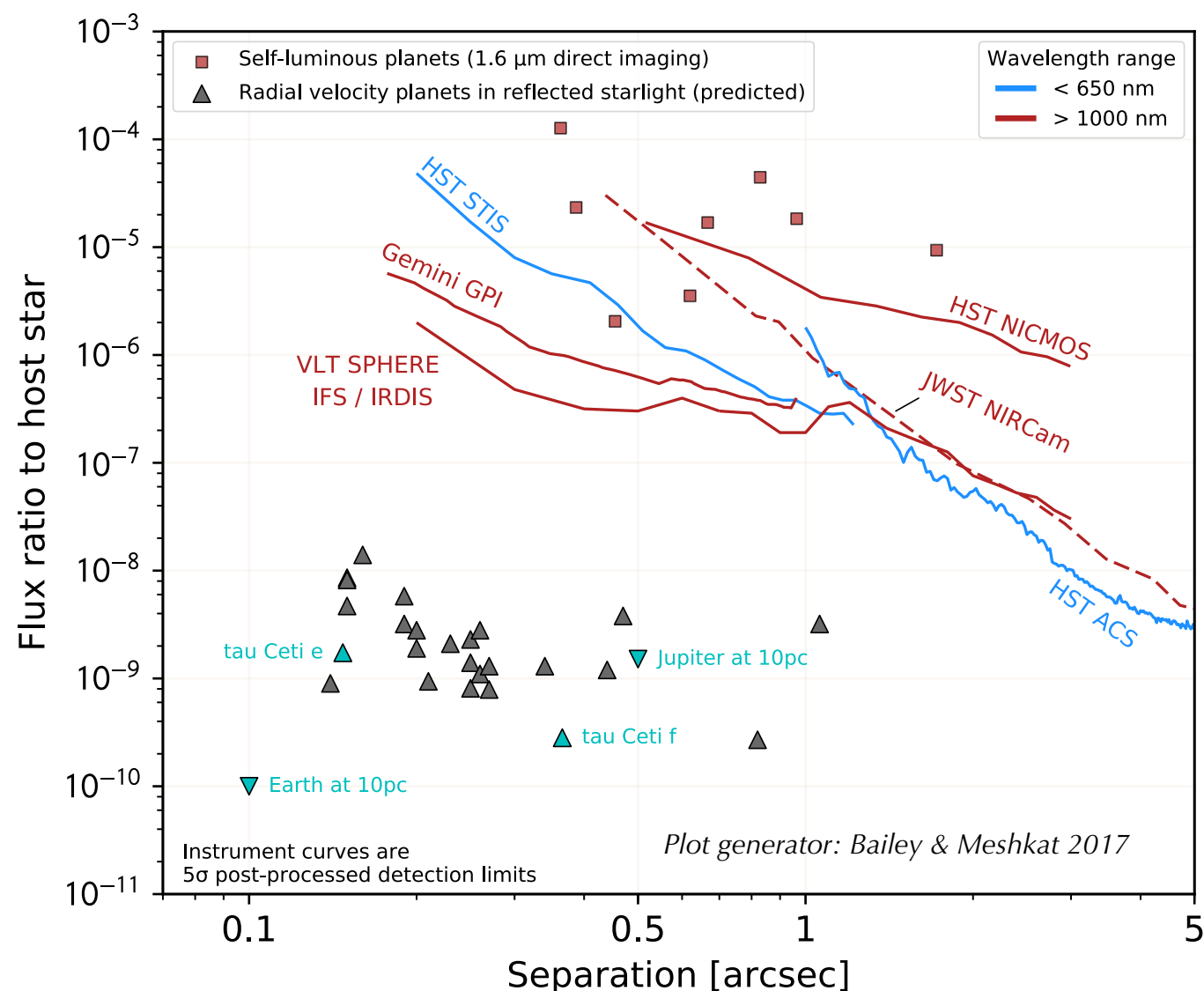
Copyright 2018, California Institute of Technology. Government sponsorship acknowledged.

The WFIRST Coronagraph Instrument

- *CGI is a technology pathfinder (2020s) for future exo-Earth imaging mission concepts, such as HabEx and LUVOIR (2030s).*
- *First reflected light images and spectra of Jupiter analogues.*
- *Potential for imaging planets in the habitable zones of nearby stars.*
- *Imaging dust belts to build a complete picture of planetary systems.*
 - *From habitable zone dust to analogues of our Kuiper belt*
 - *From epoch of planet formation to mature systems*

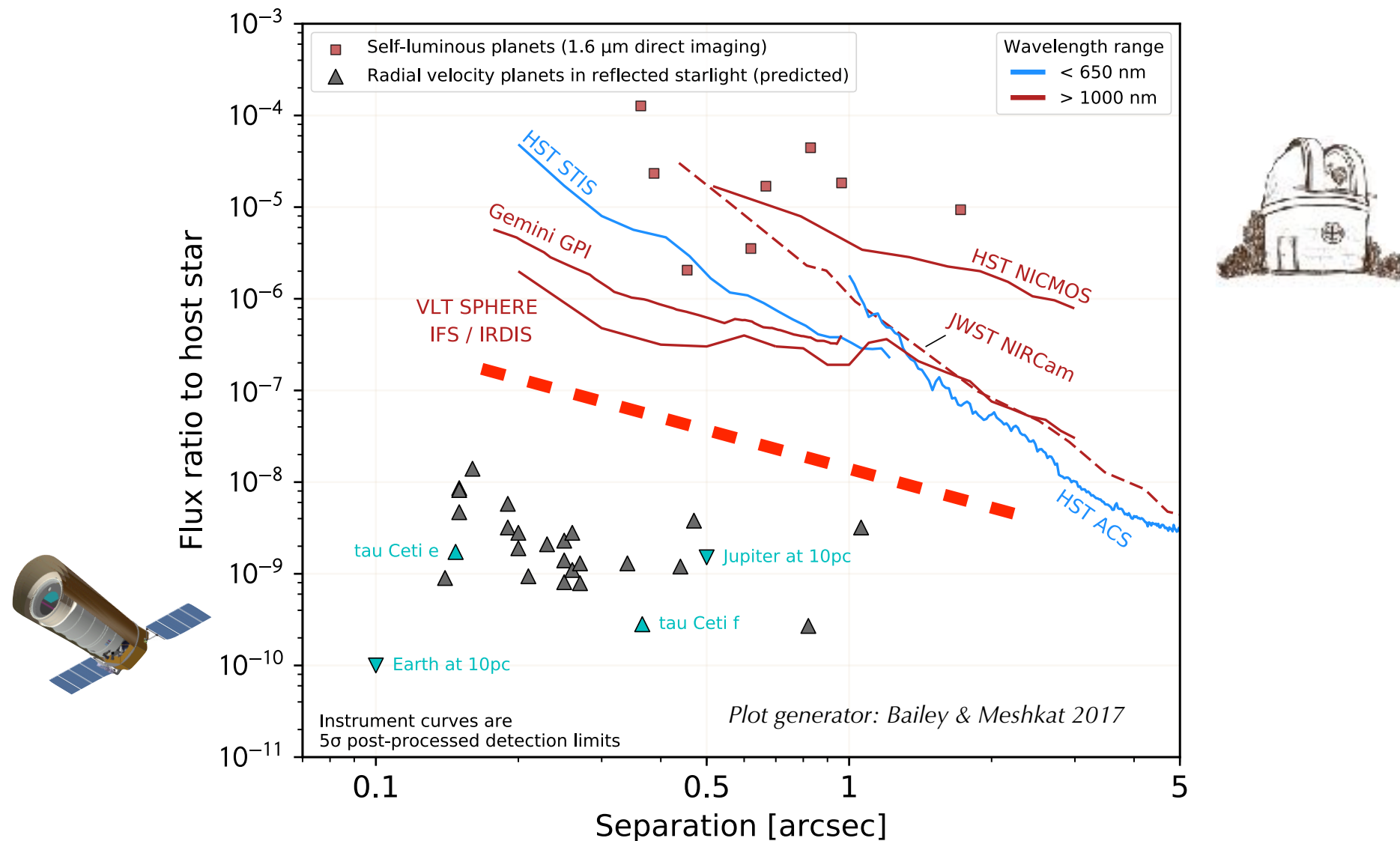


Direct Imaging of Exoplanets: 2018



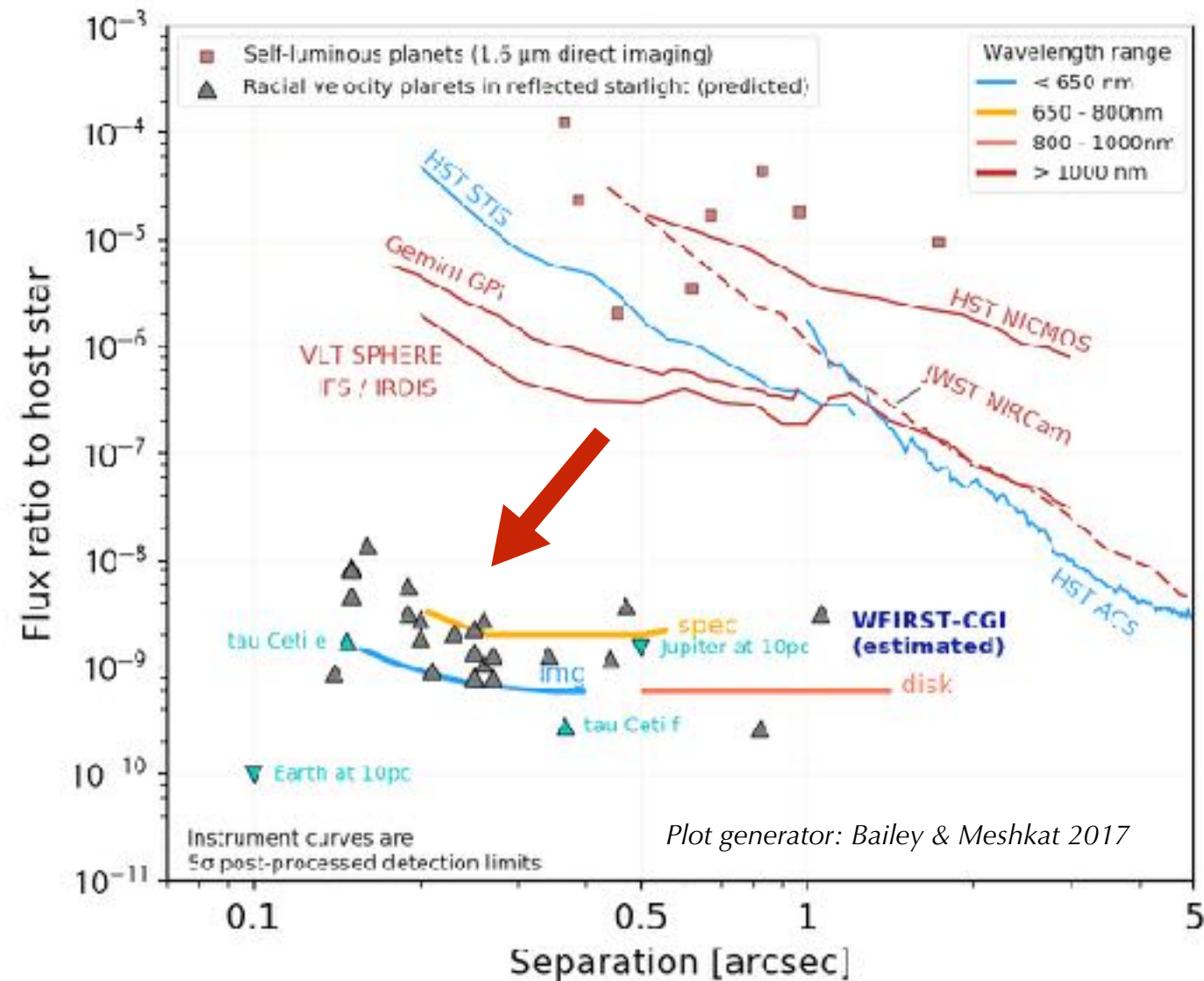
Direct imaging and spectroscopy of **young self-luminous exoplanets** have been achieved from ground and space observatories. Direct imaging of **mature cool exoplanets in reflected starlight** is currently beyond the reach of conventional techniques, as illustrated by the estimated brightness of a sample of known radial velocity exoplanets.

The *WFIRST* Coronagraph Instrument relies on the stability of a space observatory



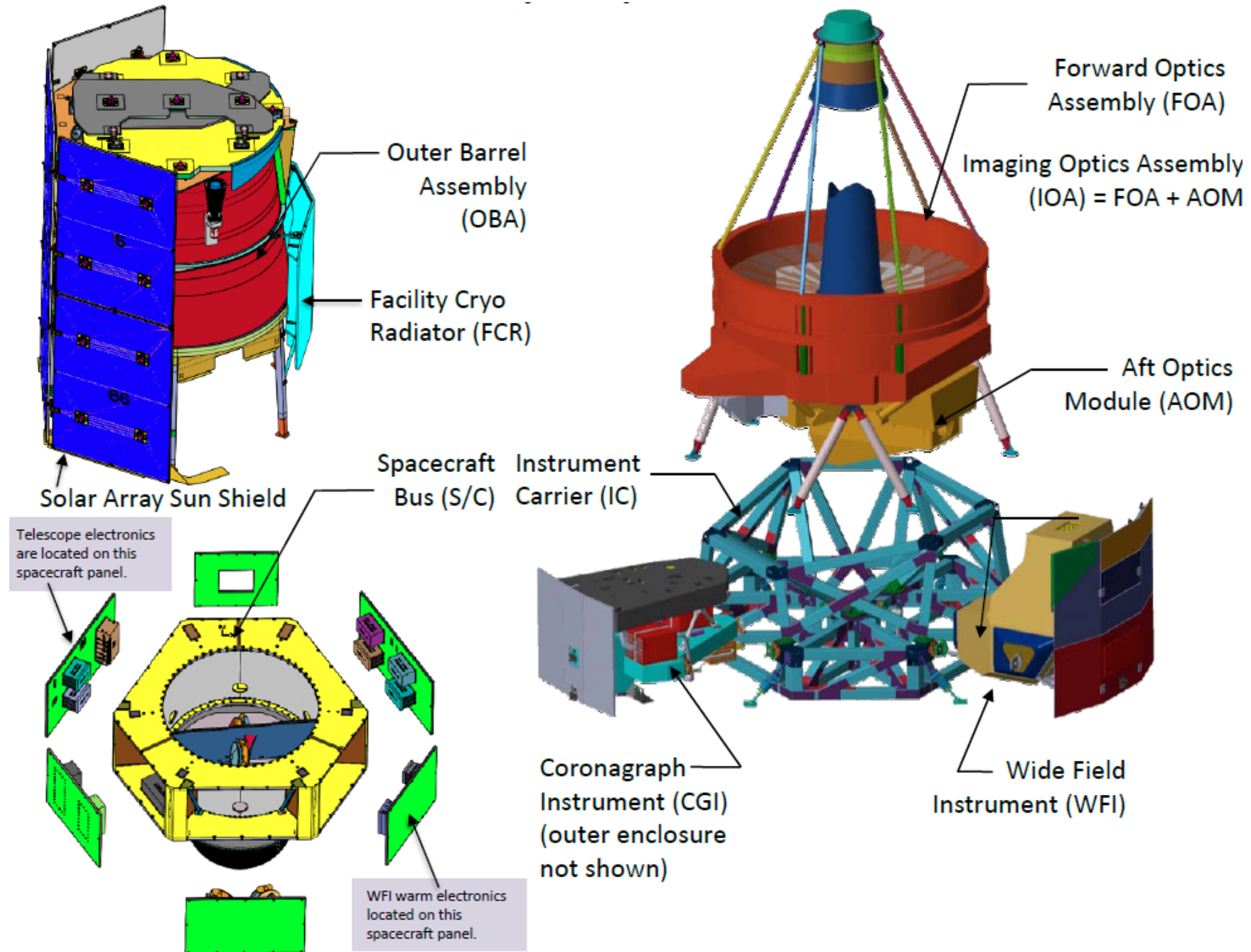
Ground-based AO systems correct the rapid phase-dominated wavefront errors due to atmospheric turbulence. Freedom from atmospheric turbulence enables the **iterative correction of both phase and amplitude wavefront aberrations** and the suppression of scattered and diffracted light to levels limited by telescope and instrument stability.

WFIRST-CGI pioneers space coronagraph technologies



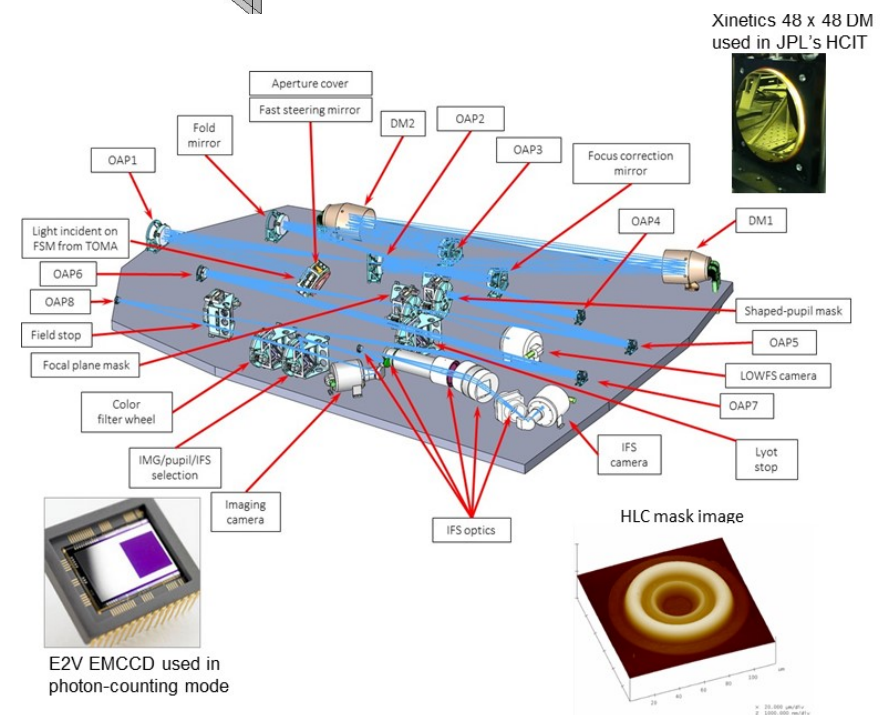
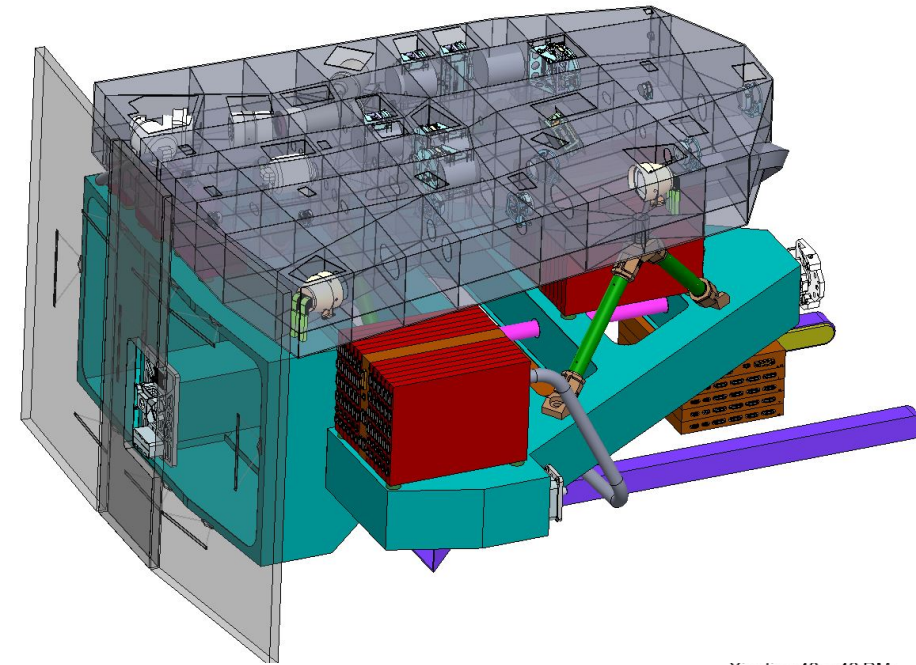
Early estimates of the CGI flux ratio curves for three observing configurations (direct imaging at short and long wavelengths, and integral field spectroscopy) are based on currently demonstrated static and dynamic testbed performance and observatory optical disturbance models provided by the WFIRST project.

CGI engineering design



CGI engineering design

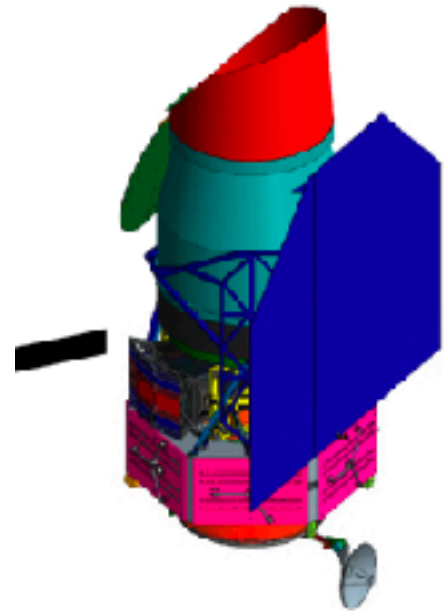
- *WFIRST is entering Phase B development:*
- *Scope of work is well understood*
- *New technology development is nearing completion, with provisions for additional technology infusion*
- *Design is validated and executable*
- *Implementation plans are in place.*



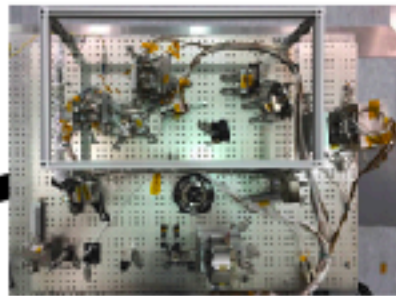
CGI incorporates critical new technologies



Large Ultra-stable Space Telescope & Observatory



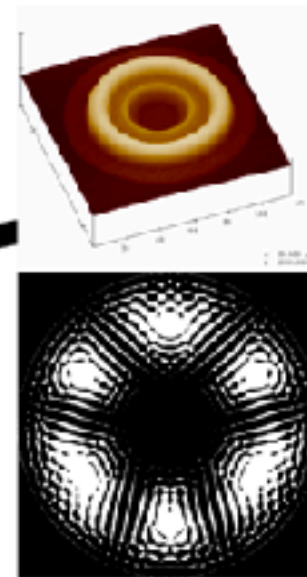
Autonomous Ultra-Precise Wavefront Sensing & Control System



First Use of Deformable Mirrors in Space



High Contrast Coronagraph Masks



Ultra-low Noise Photon Counting Visible Detectors

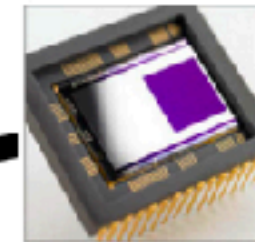
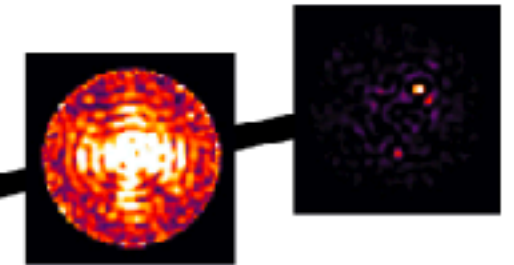
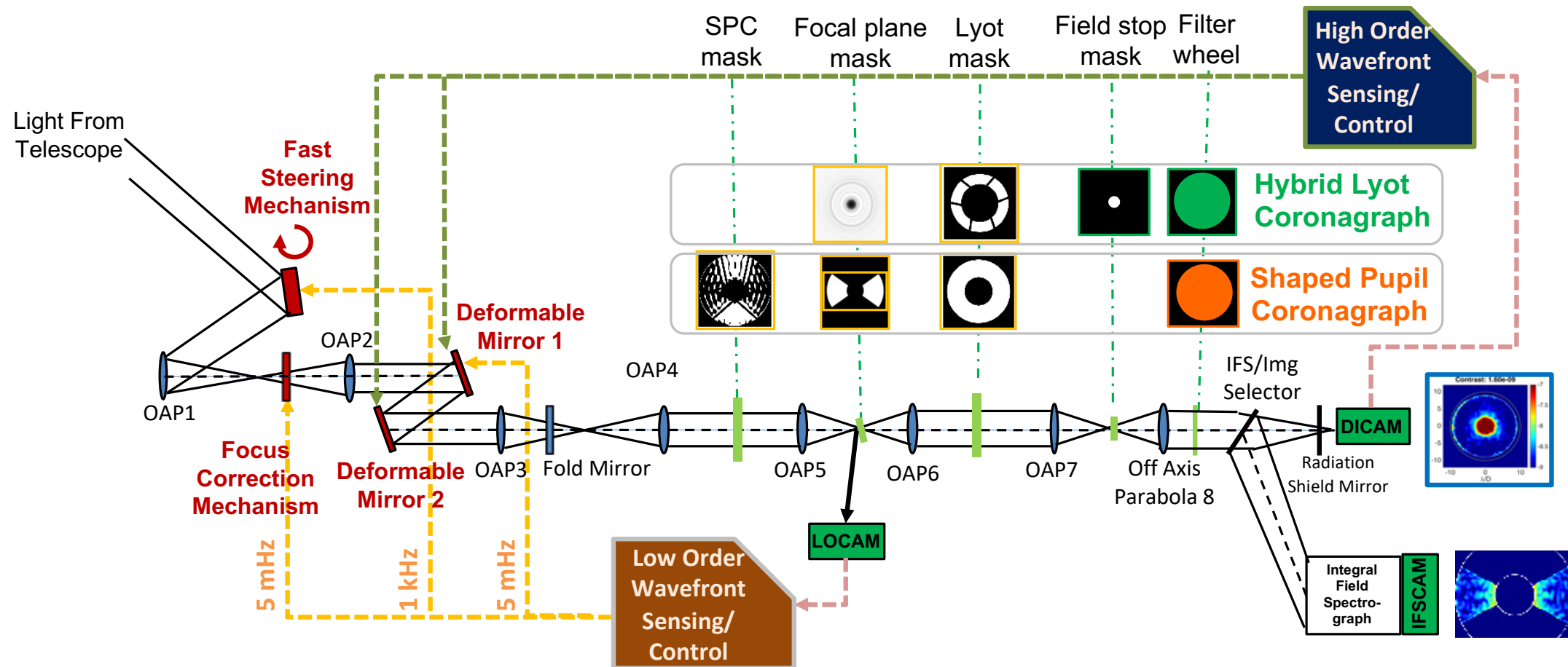


Image Processing at Unprecedented Contrast Levels



- *CGI will demonstrate in space many key technologies required for the characterization of rocky planets in the Habitable Zone, retiring significant technical risk for future potential missions such as HabEx and LUVOIR.*
- *CGI is a direct and necessary predecessor to these potential missions, and is a crucial step in the exploration of planetary systems orbiting Sun-like stars.*

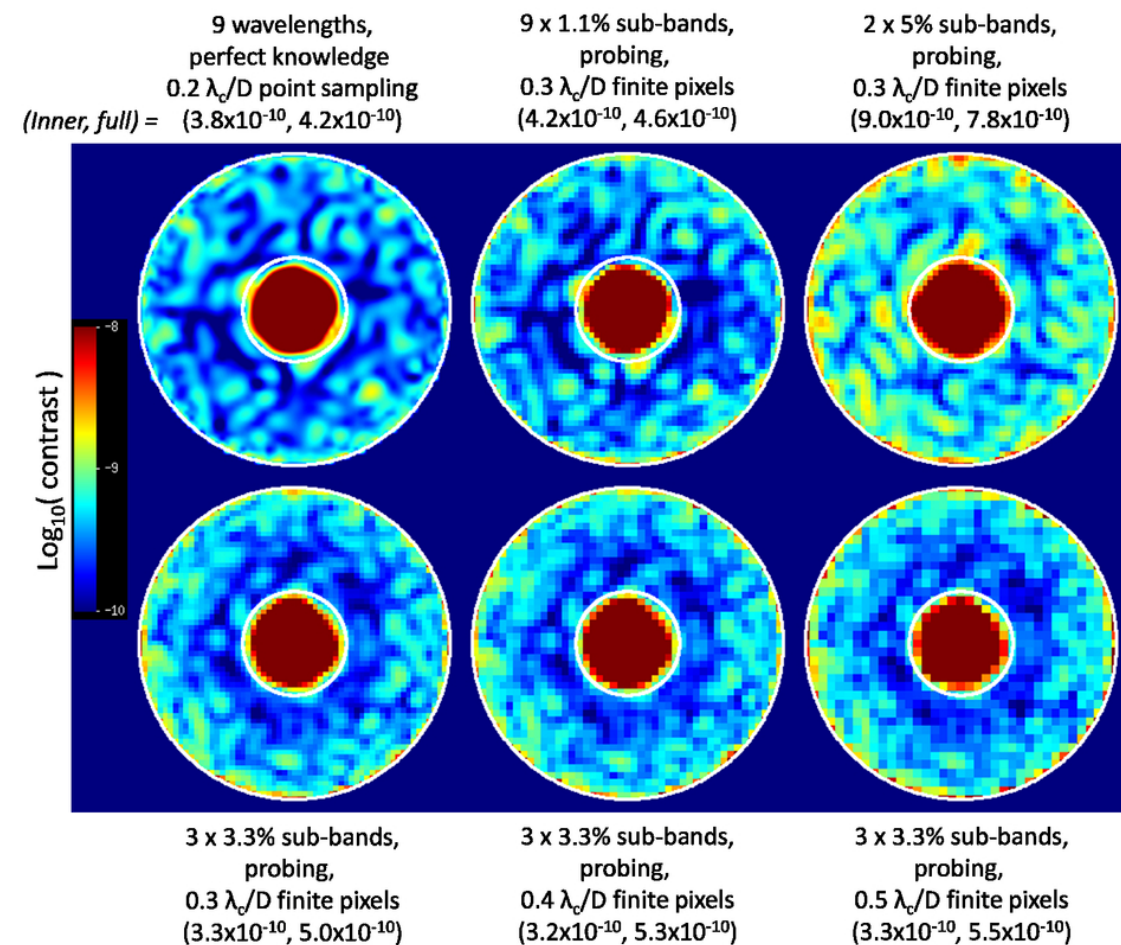
CGI optical layout enables multiple observing modes



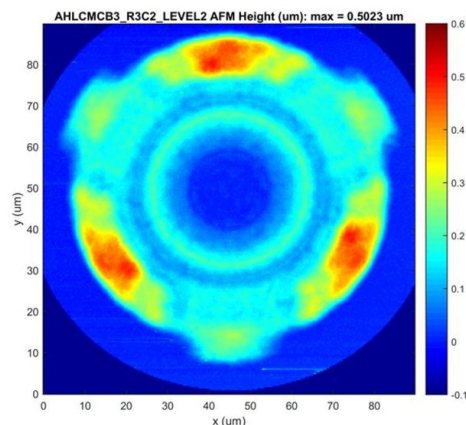
- Two selectable coronagraph technologies (HLC, SPC)
- Active wavefront control with a pair of Deformable Mirrors
- Internal LOS Pointing and Low-Order Wavefront Sensing & Control
- Direct Imaging Camera
- Integral Field Spectrograph ($R = 50$)
- Photon-Counting EMCCD detectors

The Hybrid Lyot Coronagraph

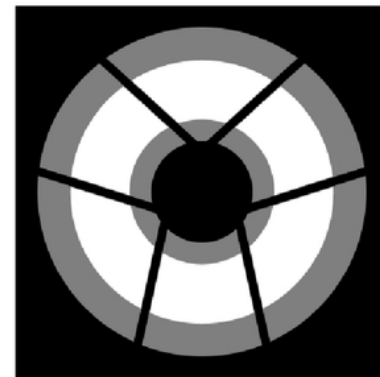
- The HLC design incorporates a numerically optimized, static actuator pattern applied to both deformable mirrors.
- Occulting mask is a $r = 2.8 \lambda_c/D$ partially-transmissive nickel disc overlaid with a radially-and-azimuthally varying dielectric coating.
- Lyot stop is an annular mask that blocks the telescope pupil edges and struts.
- 2017 design PSF core throughput is 4.5% relative to the energy incident on primary mirror (ignoring losses from reflections and filters).



Simulated HLC PSF including aberrations and high-order wavefront control operations, illustrating the annular dark zone between 3 and 9 λ_c/D . Each sub-panel represents a different scenario for DM probe wavelength resolution and detector sampling.



HLC occulting mask. Surface height measurement of an occulting mask fabricated by the JPL Micro Devices Lab. Recent design iterations like the one shown here utilize an azimuthally varying dielectric profile.



HLC Lyot stop. Diagram of Lyot stop model: white represents the transmitted region; black represents the telescope pupil; gray represents the region blocked by the stop in addition to the telescope pupil.

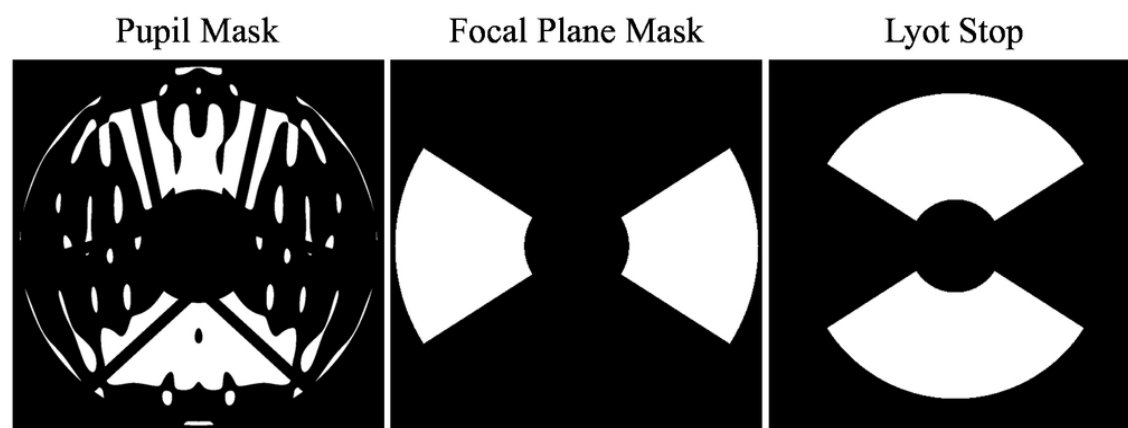
J. Trauger, D. Moody, et al., JATIS Vol 2, id. 011013 (2016) - <https://doi.org/10.1117/1.JATIS.2.1.011013>

J. Krist, et al., Proc SPIE Vol 10400, id. 1040004. (2017) - <http://dx.doi.org/10.1117/12.2274792>

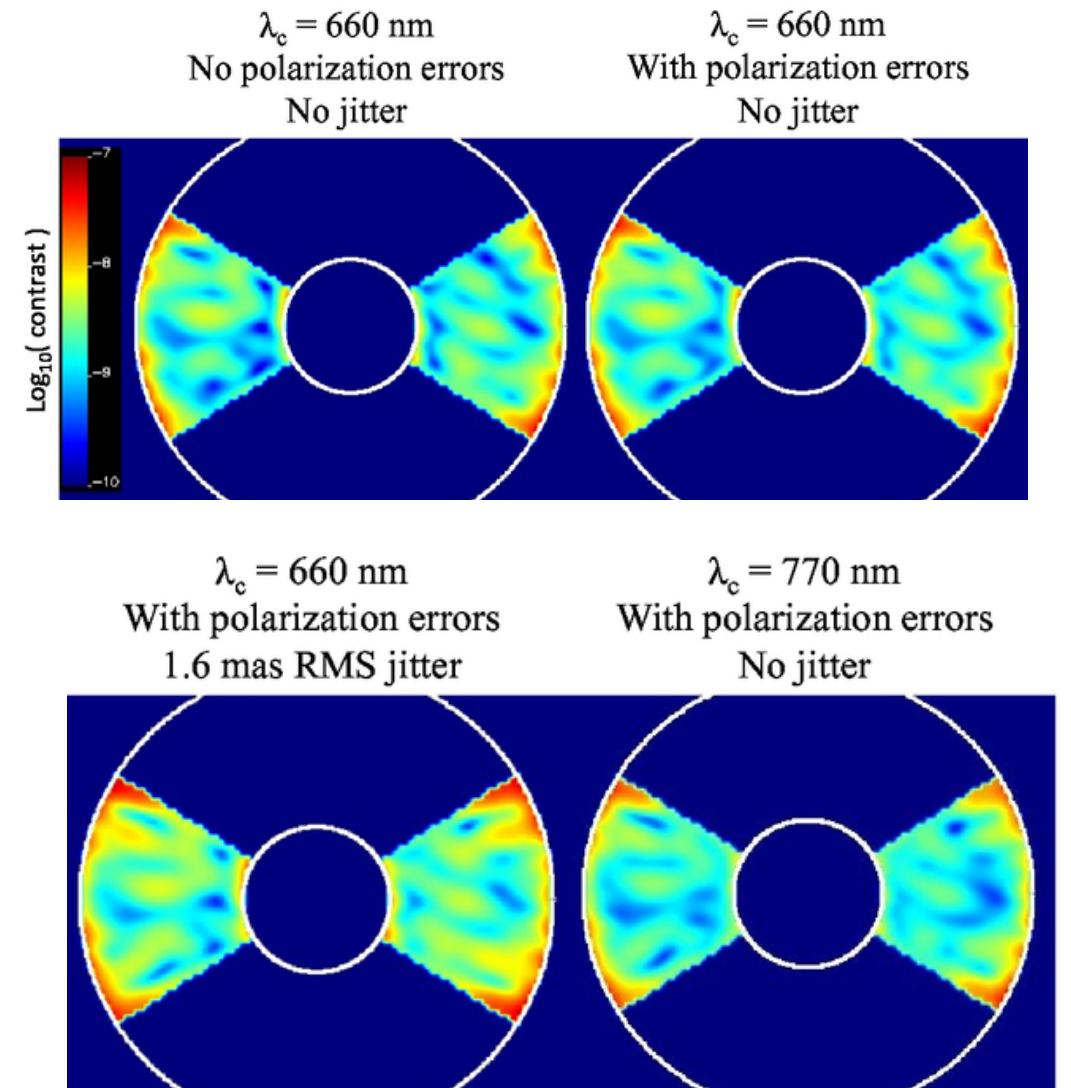
K. Balasubramanian, et al., Proc SPIE Vol 10400, id. (2017) - <https://doi.org/10.1117/12.2274059>

The Shaped Pupil Coronagraph

- The shaped pupil apodizer is a reflective mask on a black silicon substrate.
- The occulting mask is a hard-edged diaphragm with either a bowtie-shaped or annular aperture, depending on whether the characterization (spectroscopy) or debris disk shaped pupil is selected.
- The Characterization SPC designed in 2017 produces a $2 \times 65^\circ$ bowtie dark zone from $3 - 9 \lambda_c/D$ over an 18% bandpass, and has a PSF core throughput of 4.3% relative to the energy incident on primary mirror (ignoring losses from reflections and filters).
- The Debris Disk SPC design produces a 360° dark zone from $6.5 - 20 \lambda_c/D$ in a 10% bandpass.



Characterization shaped pupil coronagraph masks. 2017 design by A. J. E. Riggs.



Characterization SPC simulations at $\lambda_c = 660$ and 770 nm including system aberrations, pointing jitter, and wavefront control operations. The circles correspond to $r = 3$ and $9 \lambda_c/D$.

N. T. Zimmerman, et al., JATIS Vol 2 id. 011012 (2016) - <http://dx.doi.org/10.1117/1.JATIS.2.1.011012>

K. Balasubramanian, et al., JATIS Vol2 id. 011005 (2015) - <https://doi.org/10.1117/1.JATIS.2.1.011005>

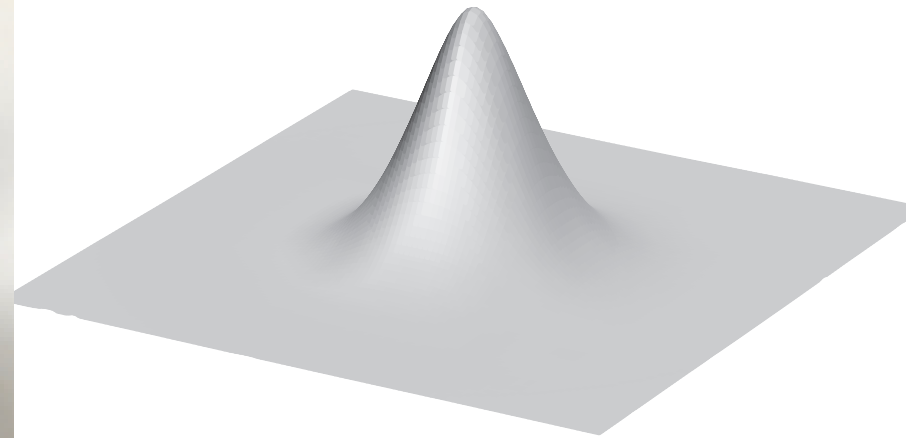
A. J. E. Riggs et al., N. T. Zimmerman, et al., Proc SPIE Vol 104000O (2017) - <http://dx.doi.org/10.1117/12.2274437>

J. Krist, et al., Proc SPIE Vol 10400, id. 1040004. (2017) - <http://dx.doi.org/10.1117/12.2274792>

Ultra-precision wavefront control technology



*Xinetics 48x48 DM
(2304 actuators on a 1x1-mm pitch)*



Single actuator influence profile

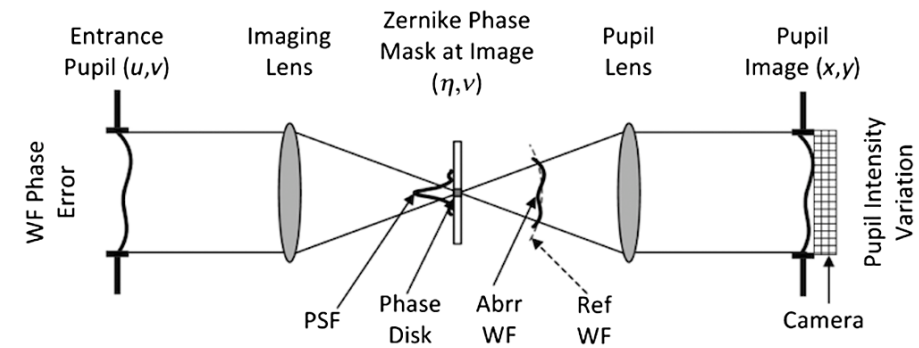


*The Vacuum Surface Gauge
interferometer provides a flight-like
environment for DM
characterizations*

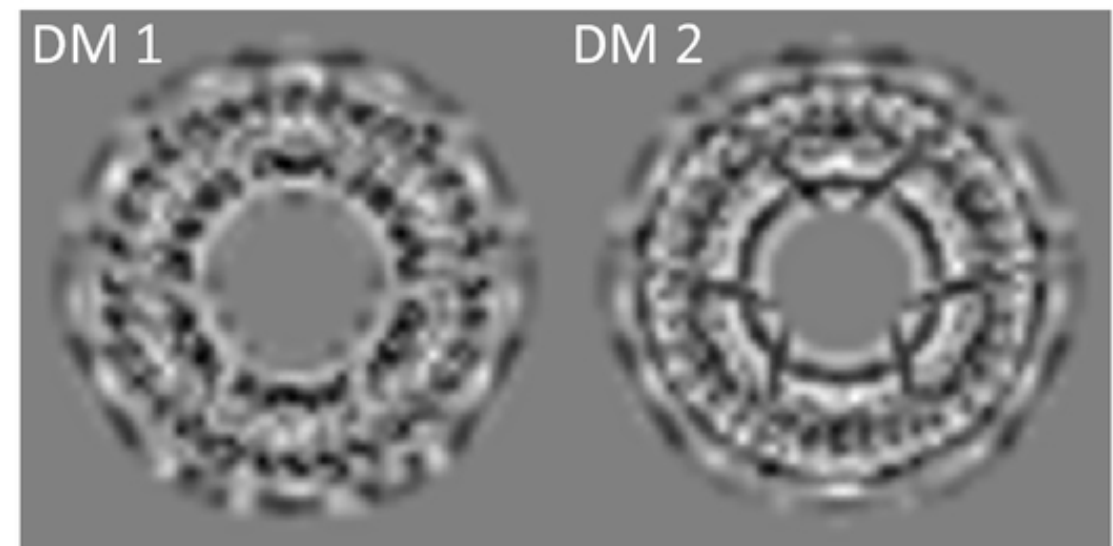
- A pair of DMs provide control over both amplitude and phase of the optical wavefront, as required for the suppression of starlight diffracted by telescope obscurations, and for the creation of the dark field of view at $\sim 1e-9$ contrast levels.*
- In addition, the DMs correct for static wavefront error in the telescope and instrument optics, and participate in the correction of thermal drift in the telescope system.*
- Laboratory demonstrations are ongoing, leading to flight qualification of the first precision deformable mirrors in a space observatory.*

CGI wavefront sensing and control

- The baseline CGI design includes 4 active optics to control the wavefront: a fast steering mirror (FSM), a flat focusing mirror (FocM), and two deformable mirrors (DM 1 and DM 2) with 48x48 actuators each.
- High-order wavefront control is implemented by the Electric Field Conjugation (EFC) method. The EFC loop operates on science focal plane data by measuring the interaction of aberrated on-axis starlight with a sequence of DM actuator probes.
- Pointing, focus, and low-order wavefront drifts are sensed by the Low-Order Wavefront Sensing and Control (LOWFS/C) subsystem using the Zernike phase-contrast technique on starlight rejected from the occulting mask. Corrections to Zernike modes Z5—Z11 are applied to DM 1 with an update interval on the order of 100 sec.
- The FSM control loop operates at 1 kHz to correct line-of-sight pointing jitter to below 1 milliarcsec.



Conceptual diagram of the Zernike phase contrast low-order wavefront sensor (F. Shi, et al., 2016).



Optimized DM surfaces applied in HLC simulations.

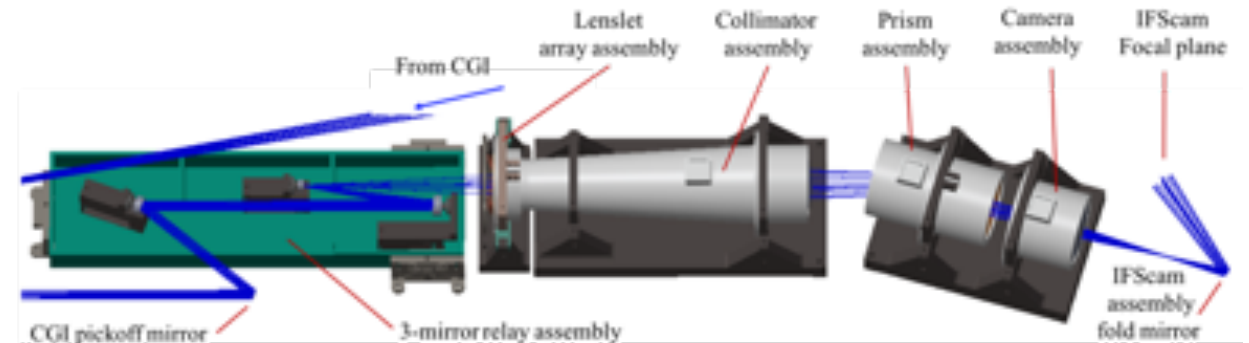
T. Groff, A. J. E. Riggs, et al., JATIS Vol 2, id 011009 (2015) - <https://doi.org/10.1117/1.JATIS.2.1.011009>

F. Shi, et al., JATIS Vol 2, id 011021 (2016) - <https://doi.org/10.1117/1.JATIS.2.1.011021>

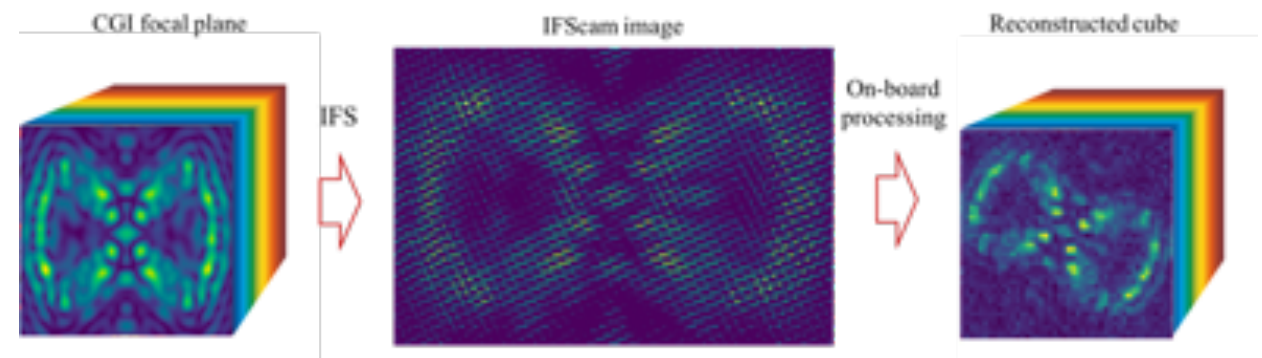
J. Krist, et al., JATIS Vol 2, id 011003 (2015) - <https://doi.org/10.1117/1.JATIS.2.1.011003>

Integral Field Spectrograph

- *Lenslet-based integral field spectrograph (IFS) with $R=50$ spectral resolving power and a 1.6-arcsec field of view.*
- *A reflective relay feeds a lenslet array, which critically samples the coronagraph image (2 lenslets per λ_c/D at 660 nm). The light from each spatial element is dispersed by a prism group.*
- *The prioritized spectroscopy demonstration filter is an 18% bandpass centered at 760 nm (CGI Science Band 3) matched to the characterization SPC. However, by design the IFS can capture an instantaneous bandpass up to 20% anywhere in the range 600 to 1000 nm.*



Baseline opto-mechanical layout of the CGI IFS, showing the beam progression through the relay mirrors, lenslet array, collimator, prism, and reimaging optics. The spectra are focused on a dedicated EMCCD detector (the IFScam; not shown).



The IFS produces a spectrally dispersed map of the CGI focal plane, comprised of a grid of interleaved microspectra. There is one microspectrum for each lenslet, or spatial element (center). A wavelength-resolved data cube (right hand side) is reconstructed by software.

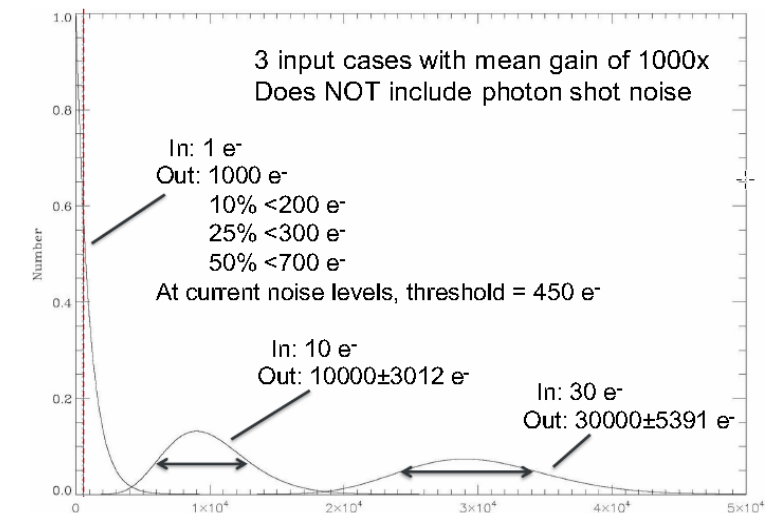
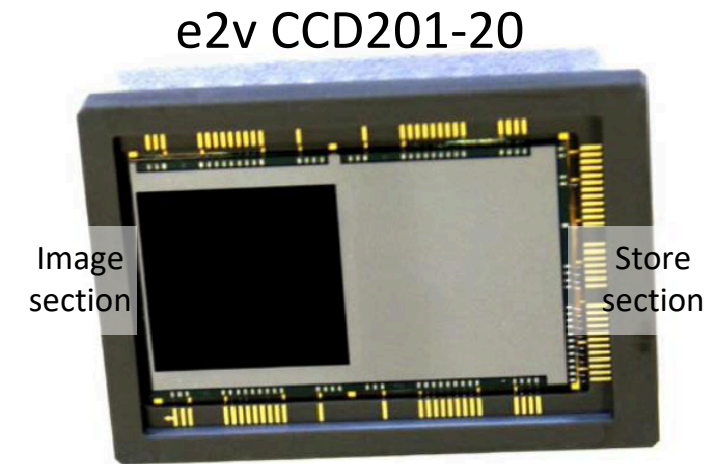
M. McElwain, A. Mandell, Q. Gong, et al., Proc SPIE Vol 9904 (2016)

M. Rizzo, T. Groff, N. Zimmerman, et al., Proc SPIE Vol 10400 (2017)

A. Mandell, T. Groff, Q. Gong, et al., Proc SPIE Vol. 10400 (2017)

EMCCD Detectors

- *Electron Multiplying CCDs are advantageous for observing very low flux sources like directly imaged exoplanets. They rely on avalanche multiplication of collected charge to greatly reduce read noise as compared to conventional CCDs. EMCCD detectors are baselined for both the Direct Imaging and IFS cameras on CGI.*
- *A Pre-Phase-A technology development effort led by JPL accelerated the maturity of e2v's CCD201-20 EMCCD for space flight. This included radiation environment testing, performance optimization, and thermal environment testing.*
- *CGI exposure time calculations incorporate models of charge traps and transfer inefficiency cause by radiation displacement damage.*
- *JPL's EMCCD test lab has measured sensitivity thresholds before and after a radiation displacement damage dose (DDD):*
 - *Beginning of life: 0.002 e-/pixel/frame for 3x3 pixel PSF, equivalent to detection of a 35th mag star using WFIRST telescope without the coronagraph.*
 - *After > 6 years radiation damage at L2: 0.007 e-/pixel/frame for 3x3 pixel PSF*



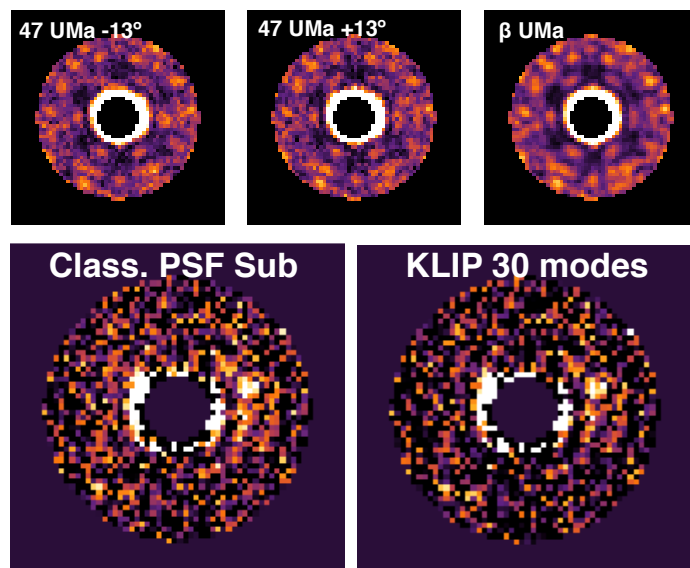
CGI will operate its EMCCDs in photon counting mode. By thresholding the readout charge values to register each pixel as either 0 or 1 photoelectrons, the 1.4x excess noise factor that originates in the uncertainty of the avalanche multiplication gain is eliminated.

L. Harding, R. Demers, et al., [JATIS Vol 2 011007 \(2016\)](#).

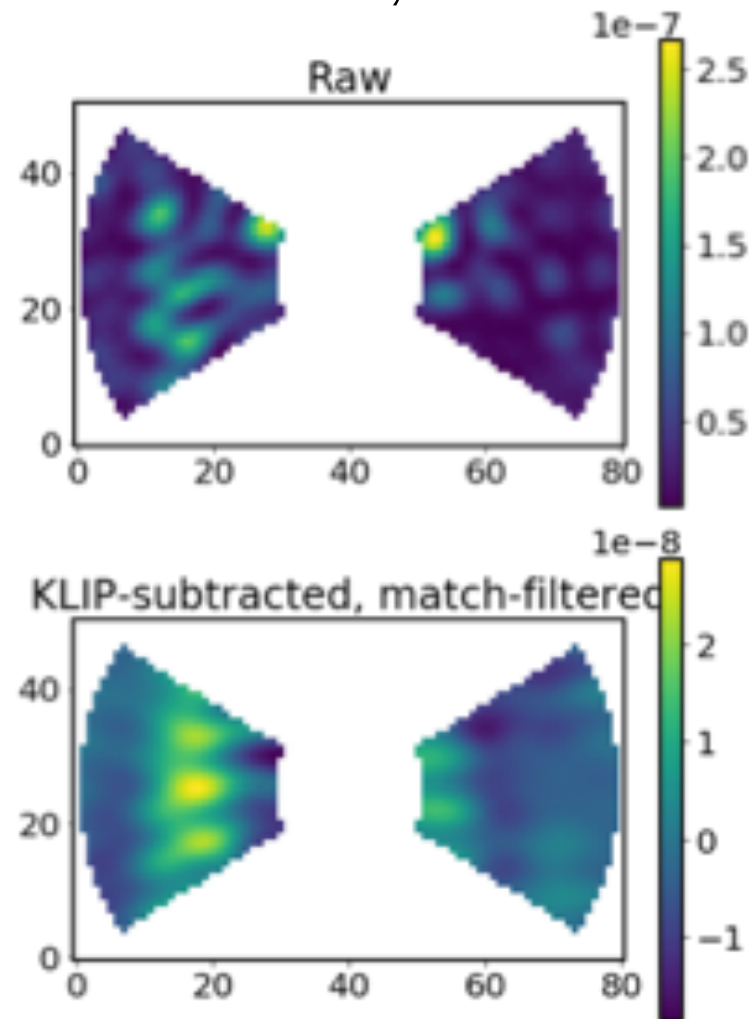
Data Post Processing

- Investigations on algorithms for CGI data post-processing have encompassed both end-to-end data simulations and analysis of laboratory testbed data.
- Reference differential imaging (RDI) trials have probed a range of wavefront stability and noise scenarios.
- Simulations with spacecraft rolls have also enabled tests of Angular differential imaging (ADI).

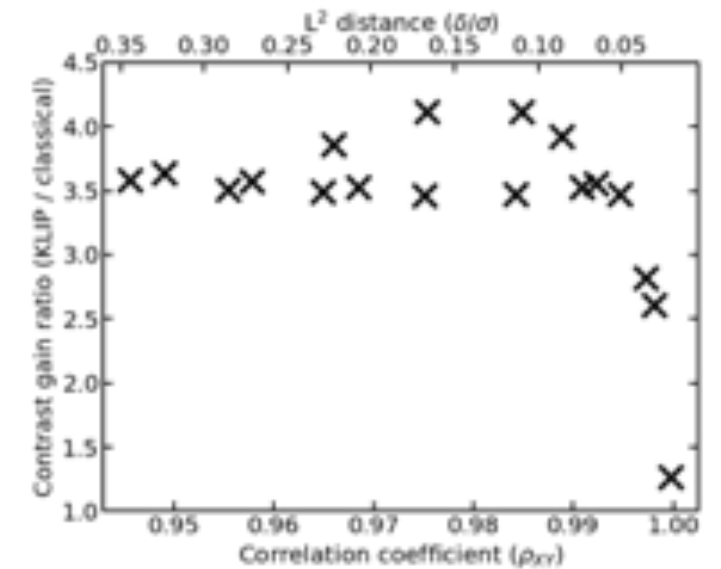
1. Post-processing trials on HLC data simulations



2. Post-processing trials on Laboratory Data



Example application of RDI to SPC data from the OMC testbed, demonstrating the match-filtered recovery of a fake point source inserted into one image.



The enhancement provided by PCA-based algorithms like KLIP depends on the level of correlation between the speckle patterns in the science image and the reference library.

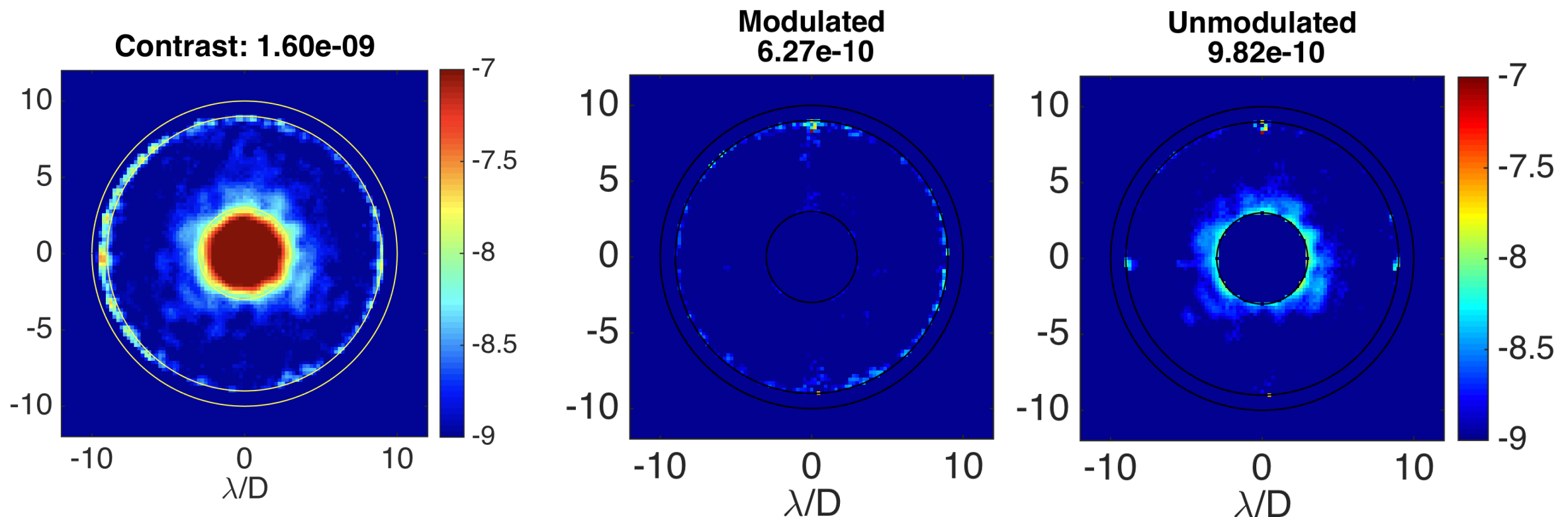
M. Ygouf, N. Zimmerman, L. Pueyo, R. Soummer, et al., Proc. SPIE Vol 9904 (2016) - <http://dx.doi.org/10.1117/12.2231581>

M. Ygouf, et al., WFIRST-STScI-TR1605 (2016) - <http://www.stsci.edu/wfirst/technicalreports/WFIRST-STScI-TR1605.pdf>

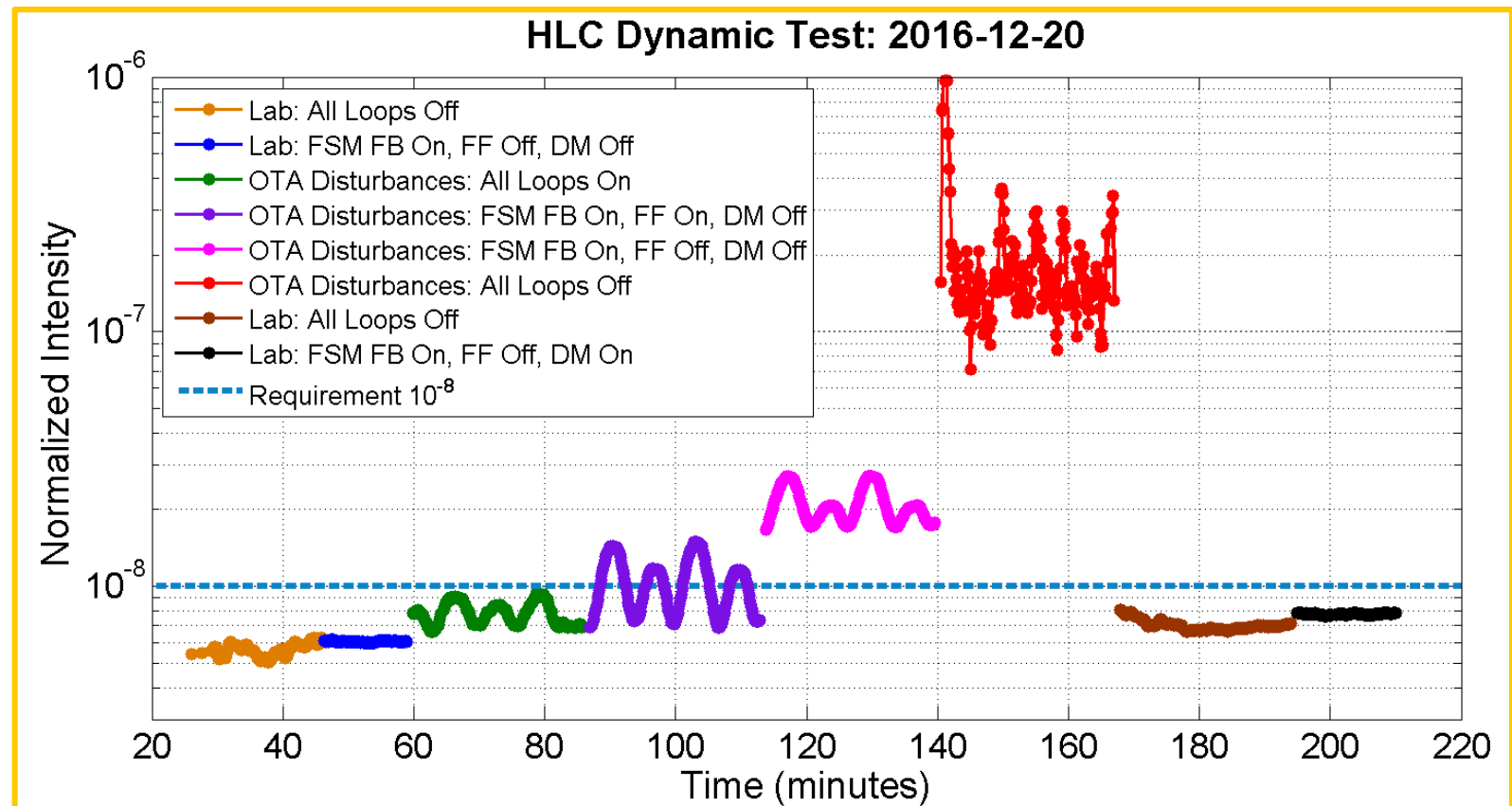
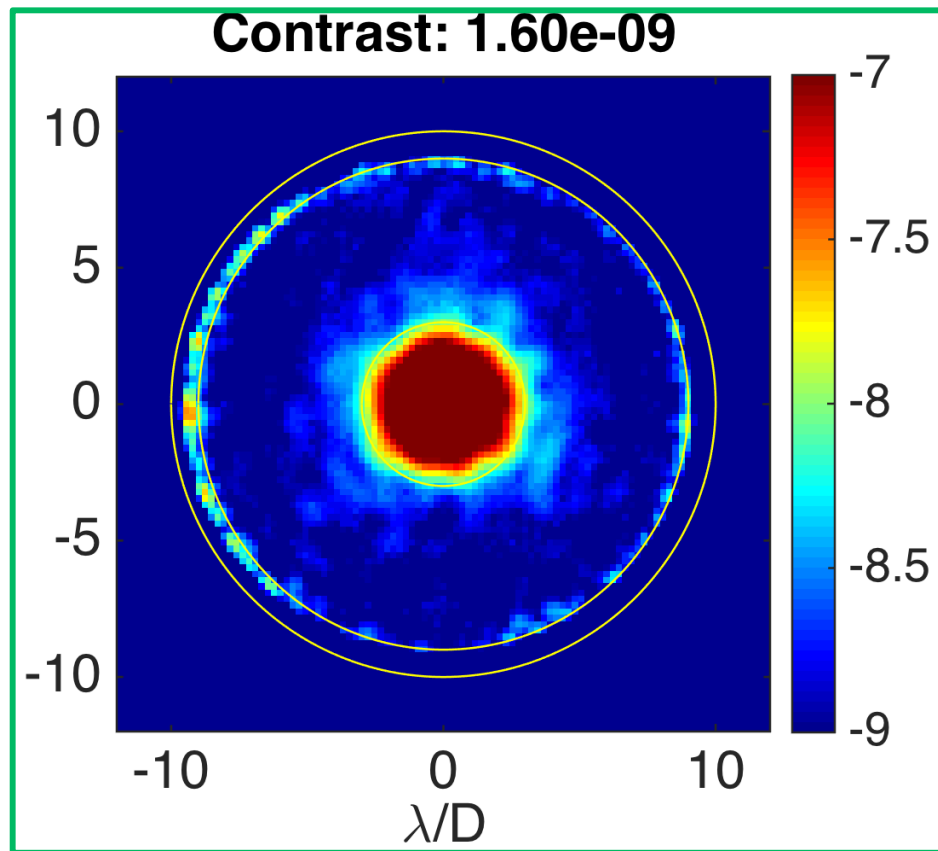
M. Ygouf, et al., WFIRST-STScI-TR1601 (2016) - <http://www.stsci.edu/wfirst/technicalreports/WFIRST-STScI-TR1601.pdf>

Laboratory high contrast demonstrations

- Static testbed **HLC performance** (550 nm, 10% bandwidth) as of 12/2016 (J. Seo et al.).
- A significant fraction of the light (at the inner working angle in particular) is not sensed (unmodulated) by the EFC probing.
- **Discrepancies between predicted and measured contrast and tolerances** to tip/tilt errors:
 - Are unlikely to be fabrication errors in the coronagraph masks.
 - Are most likely dominated by errors and drift in optics alignments, testbed jitter, and DM calibration.
- **Calibration of the DMs** can be improved as part of an effort to improve validated testbed performance, including static contrast, tolerance to wavefront errors, and EFC convergence rates.

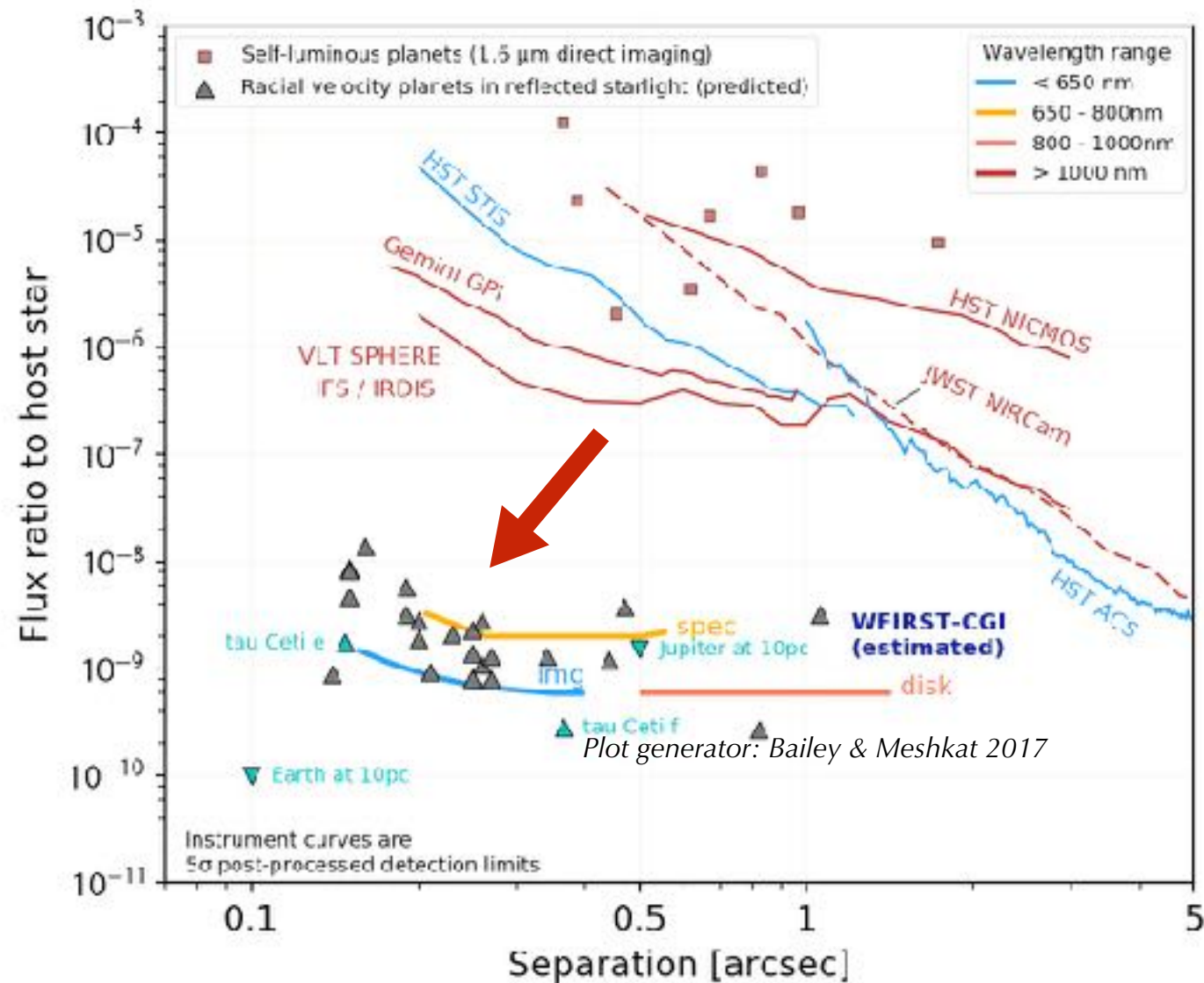


Laboratory wavefront control demonstrations



- HLC contrast laboratory demonstration on the WFIRST MCB testbed: 10% spectral bandwidth centered at 550 nm.
- At left, a **demonstration of 1.6×10^{-9} contrast** in the MCB testbed (J. Seo, 12/2016).
- At right, **contrast in the dynamic testbed environment** simulating on-orbit pointing and focus disturbances, and LOWFS&C sensing and rejection (F. Shi, 12/2016): 14 mas rms pointing drift plus estimated WFIRST jitter corrected with a fast steering mirror; 2 nm PV focus disturbance (4x worst than WFIRST expectations) corrected with the DM.

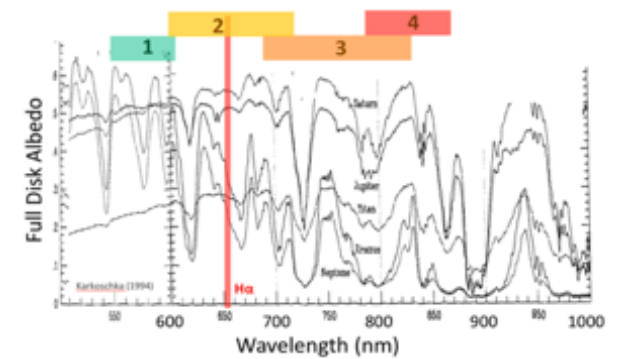
WFIRST-CGI pioneers space coronagraph technologies



Early estimates of the CGI flux ratio curves for three observing configurations (direct imaging at short and long wavelengths, and integral field spectroscopy) are based on currently demonstrated static and dynamic testbed performance and observatory optical disturbance models provided by the WFIRST project.

Baseline 18-month space technology demonstration

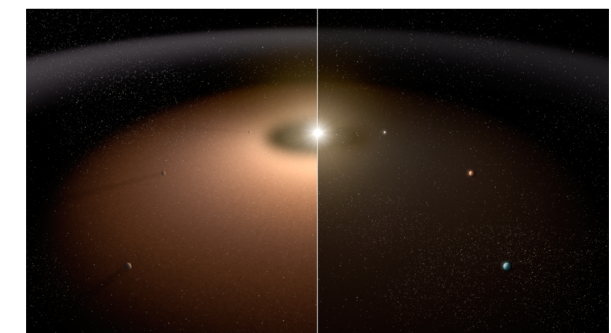
- Spectra of ~2 young, self-luminous super-Jupiters
 - Beta Pic b, HR 8799 e, 51 Eri b
- Masses for ~10 Jupiter analogues
 - Direct imaging breaks $v \sin(i)$ degeneracy in mass of RV planets
- Spectra of a 1-2 Jupiter analogues
- Circumstellar disks
 - Image 2-4 bright, known debris & protoplanetary disks
 - More details of inner regions; new wavelengths
 - First images of 1-2 (faint) exozodi disks



First images and spectra of reflected visible light from Jupiter analogs.



Explore the nature of the HZ planets orbiting Tau Ceti.



Interplanetary dust in the HZ of Sun-like stars:
- evolution of planetary systems
- prepare for future exo-Earth imaging missions

Additional 1.25 years over 5 years

To be guided by a Participating Scientist Program

- *~double the number of planets with imaging and spectroscopy*
- *More than double the number of imaged disks*
- *~3 months for a search for new planets*
 - *Could discover ~10 new Jupiter analogues*
 - *May discover a few Neptunes or mini-Neptunes*
- *Investigate ~20 highest priority systems for exo-Earth missions*
 - *Exo-Earth imaging needs relatively “clean” (low dust) systems*
 - *Search for Jupiter analogues in systems with poor RV constraints*

Expanded science areas & possible GO program

- *New community-driven exoplanet & disk science*
- *General astrophysics, AGNs, evolved stars...*
- *Possible starshade rendezvous*

Extended mission (beyond the 5-year nominal life)

- *Continue to build on programs from first 5 years*
- *Possible starshade rendezvous*
 - *Imaging exozodi & planets in HZ*
- *Exploit and advance demonstrated high-contrast capabilities*
 - *Deep imaging of new super-Earth or mini-Neptune candidates*
 - *Deep spectroscopy of most interesting Jupiter/Saturn analogues*
 - *Opportunities for innovative GO programs*

End